22 September 2000

ELSEVIER

Chemical Physics Letters 328 (2000) 234–243

CHEMICAL PHYSICS LETTERS

www.elsevier.nl/locate/cplett

Photochromism of diarylethene derivatives in rigid polymer matrix: structural dependence, matrix effect, and kinetics

Doo-Hyung Kwon [a], Hee-Won Shin [a], Eunkyoung Kim [b], Doo Wan Boo [a,1], Yong-Rok Kim [a,*]

[a] *Department of Chemistry, Yonsei University, Shinchon 134, Seoul 120-749, South Korea*

[b] *Advanced Materials Division, Korea Research Institute of Chemical Technology, P.O. BOX 107, Yusung, Taejeon, 305-600, South Korea*

Received 20 March 2000; in final form 6 July 2000

Abstract

Photochromic reactions of three diarylethene derivatives embedded in three types of polymer matrices were studied using a variety of spectroscopic techniques and quantum ab initio computations. It was found that the photochromic efficiencies of diarylethene molecules depend on the structural and electronic characteristics of Franck–Condon region in the excited states, and also depend strongly on the sizes of free inner spaces of the matrices. The steady-state and time-resolved fluorescence studies revealed the detailed kinetics of the planar and twisted conformers in the excited states. The observed fluorescence lifetimes of the planar and twisted conformers were ~ 2.6 ns and $8 \sim 30$ ns. © 2000 Published by Elsevier Science B.V.

1. Introduction

Diarylethene derivatives have been known as one of the most attractive photochromic molecules for their potential applications as rewritable optical data storage media [1–7]. Photochemical ring-cyclization and ring-opening reactions are the fundamental photochromic behaviors of the diarylethene derivatives. During last decade many spectroscopic studies on their photochromic reactions in the solution phase have been performed [8–15], and revealed that the ring-cyclization reactions take place less than ~ 10 ps in solution [10,11,14]. It was also suggested that the stabilities of the excited state conformational isomers are strongly influenced by solvent polarities, and the ring-cyclization reactions occur preferentially in nonpolar solvents due to the relatively nonpolar structures of the favorable planar isomers for ring-cyclization [9]. Despite many prior studies on the solution phase dynamics, few works on the photochromic behaviors in solid state films have been reported so far. Since the solid state thin films containing photochromic chromophores are the media for optical data storage, the studies on the photochromic reactions in the polymer matrices rather than in the solution are more desirable from the viewpoints of practical applications.

In this work, it is our goal to investigate the photochromic behaviors of three diarylethene derivatives embedded in three different types of polymer matrices, and to compare them with the results in the solution phase. Cis-1,2-bis(2-methylbenzothiophene-

* Corresponding author. Fax: +82-2-364-7050; e-mail: yrkim@alchemy.yonsei.ac.kr

[1] Fax: +82-2-364-7050; e-mal: dwboo@alchemy.yonsei.ac.kr

0009-2614/00/$ - see front matter © 2000 Published by Elsevier Science B.V.
PII: S0009-2614(00)00893-9

3-yl)-1,2-dicyanoethene (BTCN, **1a**), 1,2-bis(2-methylbenzothiophene-3-yl)maleic anhydride (BTMA, **2a**), and 1,2-bis(2-methylbenzothiophene-3-yl)per fluorocycloalkenes (BTF6, **3a**) were chosen as the benchmark systems due to the following reasons: One is that their photochromic behaviors in the solution phase have been well-characterized, so well-suitable for close comparison. The other is that they have quite different photochromic activities despite the structural resemblance, so the origin of the structural dependence of the photochromic activities is of particular interest).

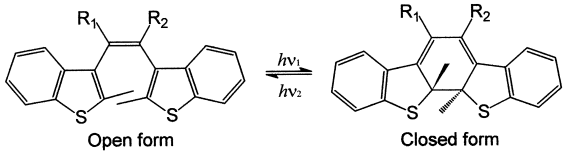

1a. BTCN : R_1=R_2=CN
2a. BTMA : R_1R_2=CO-O-CO
3a. BTF6 : R_1R_2=CF_2-CF_2-CF_2

1b. R_1=R_2=CN
2b. R_1R_2=CO-O-CO
3b. R_1R_2=CF_2-CF_2-CF_2

Three polymer matrices employed in this work are polyethylene (PE), polymethylmethacrylate (PMMA), and Poly(ethyleneglycol)-grafted polysiloxane (PEG-g-PS). They were chosen because they possess different dielectric constants giving various polar environments for the chromophores, and also predicted to have different inner spaces for the conformational changes of chromophores.

It will be shown that the photochromic activities of diarylethene derivatives depend strongly on the Franck–Condon (FC) structures in the excited states and on the properties of polymer matrices such as their polarities and glass transition temperatures (T_g) determining the sizes of free inner spaces. Finally, the detailed kinetics and energy dynamics of the radiative processes and the ring-cyclization reactions upon S_0-to-S_1 excitations will be discussed extensively.

2. Experimental

The synthetic methods for three diarylethene derivatives used in this work have been reported previously [16,17]. All the samples were doped in the polymer matrices, and subsequently spin-coated on 5×25 mm quartz plate. Steady-state absorption and fluorescence spectra were measured with UV-VIS absorption spectrophotometer (Shimatsu, UV-160A) and fluorescence spectrophotometer (Hitachi, F-4500). Fluorescence lifetime was measured by a time-resolved fluorescence set-up with a pulsed nitrogen laser (Laser Photonics, 600 ps FWHM). The 337 nm of pulsed nitrogen laser was used for the excitation of **3a**, and 400 nm of pulsed dye laser pumped by nitrogen laser was used for **1a** and **2a**. The instrument response function (IRF) was estimated to be $\sim$2 ns (FWHM). The observed fluorescence decay curves were finally deconvoluted with multiple exponential functions by a nonlinear least squares method. The density functional ab initio computations of three diarylethene molecules were also performed at B3LYP/6-31G(d) level using the GAUSSIAN 98 and 98W packages [18].

3. Results and discussion

3.1. Photochromism: structural dependence and matrix effect

The spectral changes in the UV-VIS absorption spectra in Fig. 1 induced by the photochromic ring-cyclization reactions of **1a**, **2a**, and **3a** in PEG-g-PS matrix are shown. After $\sim$6 min irradiation at 400 nm on **1a**, **2a**, and 337 nm on **3a**, the absorption intensities at 400 and 300 nm were somewhat reduced and simultaneously a new band near 520 nm appeared for all the samples (denoted as dashed lines). Similar trends were also seen for three diarylethene molecules in other polymer matrices (not shown here).

Quantum yields of the photochromic ring-cyclization (Φ_{pc}) can be determined from the changes of absorption bands due to ring-cyclization reactions by calculating the degrees of conversion and the number of absorbed photons at the given radiation power and absorbance of the samples [19]. Table 1 summarizes the photochromic efficiencies of **1a**, **2a**, **3a** in three polymer matrices. They increase in the order of **2a** $<$ **1a** $<$ **3a** for all the matrices used, indicating possible correlation of photochromic activities with

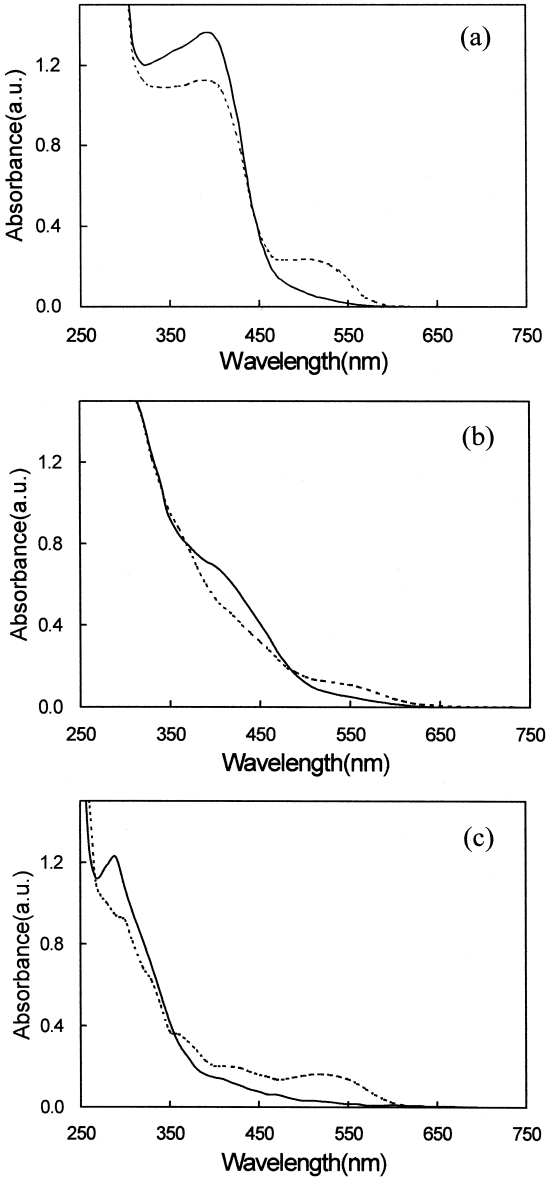

Fig. 1. Steady-state absorption spectra of (a) BTCN, (b) BTMA, and (c) BTF6 in PEG-g-PS matrix without irradiation (—) and with irradiation (- - -) at (a) 400 nm; (b) 400 nm; and (c) 337 nm.

the inherent structural properties of diarylethene molecules. It is also noteworthy that the Φ_{pc}'s of **2a** in PE and PMMA matrices with low dielectric constants were almost negligible while the Φ_{pc} of **3a** in PEG-g-PS with higher dielectric constant was highest among the nine sample-matrix combinations. These results are different from the previous results in solution phase that the Φ_{pc} decreases with the increasing solvent polarity, indicating additional environmental effects of polymer matrices besides the effects of polarities.

The origin for the marked differences in the photochromic activities is first addressed. As mentioned previously, three diarylethene derivatives possess different photochromic activities of ring-cyclization: for instance, the Φ_{pc} for **3a** in a PEG-g-PS matrix is greater than that for **1a** and **2a** by factors of 4.4 and 52, respectively. We postulated that the differences in Φ_{pc}'s may be due to their different structural and electronic properties in the excited electronic states (S_1) where the ring-cyclization reaction takes place. As a preliminary study and for simplicity, we focus in this work only on the FC region in the S_1 state where the ring-cyclization reaction starts, to seek for possible correlation between the structural and electronic characteristics and the measured Φ_{pc}'s. It was also assumed that the *cis*-hexatriene moieties (C1 ~ C6) of diarylethene derivatives represent the chromophores for $S_0 \rightarrow S_1$ transition, and the FC regions of the S_1 states accessed by π–π^* vertical transitions are approximately characterized by the lowest unoccupied molecular orbitals (LUMO) with two opposite phase p orbitals centered at C1 and C6 but with the ground state structures (see Fig. 2 for the numbering). The two p orbitals were further assumed to be perpendicular to the corresponding benzothiophene planes. This simplification alleviates greatly our computational efforts that only the ground state calculations are necessary for the purposes of the present discussion.

Table 1
Photochromic quantum yields for ring-cyclization reaction

Matrix	Φ_{pc} (BTCN,**1a**)	Φ_{pc} (BTMA,**2a**)	Φ_{pc} (BTF6,**3a**)
PE (ε [a] = 2.28)	0.013	~ 0	0.065
PMMA (ε = 3.0)	0.008	~ 0	0.032
PEG-g-PS (ε = 8.2)	0.071	0.006	0.31
λ_{irr} [b] (nm)	400	400	337

[a] Dielectric constant.
[b] Irradiation wavelength.

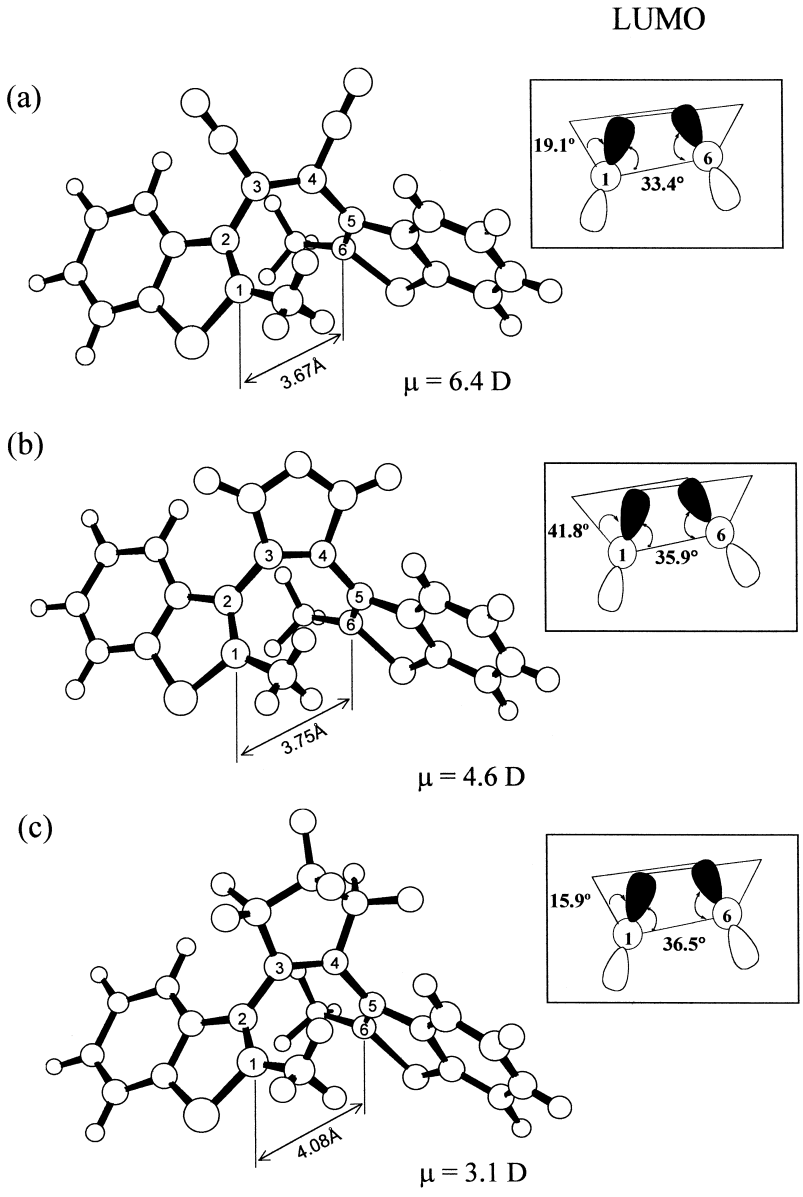

Fig. 2. The optimized ground state structures of (a) BTCN, (b) BTMA, and (c) BTF6 at B3LYP/6-31G(d) level. The orientations of two p orbitals at C1and C6 in LUMO, namely the tilted angles and the dihedral angles are also depicted.

The optimized ground state structures and the calculated geometrical parameters of two LUMO p orbitals at C1 and C6 for **1a**, **2a**, and **3a** at B3LYP/6-31G(d) level are depicted in Fig. 2 [20]. Three geometrical parameters such as the C1-C6 distance, the tilted angle of two LUMO p orbitals at C1 and C6 to the C1-C6 axis, and the dihedral angle of two p orbitals around the C1-C6 axis were examined for possible correlation with the measured Φ_{pc}'s. They are closely related to the reaction coordinates of the ring-cyclization reactions since the reactions proceed via internal rotations of two benzothiophene

rings around the C2-C3 and C4-C5 axes, resulting in the formation of a σ bond between C1 and C6 [21].

The trends of the C1-C6 distances and the tilted angles to the C1-C6 axis, however, seem to have no obvious correlation with the measured Φ_{pc}'s: For instance, 3.75, 3.67, 4.08 Å; 35.9°, 33.4°, 36.5° versus 0.006, 0.071, 0.31 for **2a**, **1a**, **3a** in a PEG-g-PS matrix. It is interesting to notice that the C1-C6 distance and the tilted angle for **3a** possessing the greatest Φ_{pc}'s are unexpectedly largest among three molecules. Conversely, the Φ_{pc}'s correlate well with the dihedral angles of two LUMO p orbitals: 41.8°, 19.1°, 15.9° for **2a**, **1a**, **3a**. Having greater Φ_{pc}'s for smaller dihedral angles can be understood from the fact that the two LUMO p orbitals with smaller dihedral angles would be able to form σ bond more easily than those with larger dihedral angles due to the less conformational changes needed for the orbital overlap. These findings may suggest an important role of the dihedral angle of two LUMO p orbitals in determining the photochromic activities of diarylethene derivatives.

From Table 1, it is seen that the Φ_{pc}'s in the polymer matrices are much smaller compared to those in the solution phase [6], and also depend strongly on the types of matrices used. Another fact to notice is that the Φ_{pc}'s in PEG-g-PS are greater than those in PE and PMMA despite its large dielectric constant, different from the trends observed in the solution phase. The combined results suggest that beside the polarity effects there may exist environment effects of the polymer matrices by their confined inner spaces that could hinder significantly the conformational changes involved in the photochromic reactions. Among various physical parameters of polymer matrices, their glass transition temperatures (T_g) may be correlated with the rotational freedom of the chromophores inside the polymer matrices. The sizes of free inner spaces of polymers may decrease with the increasing T_g [22]. The T_g of PE, PMMA and PEG-g-PS are -20°C, 105°C, and -65°C, respectively [23], indicating the sizes of the inner spaces in the order of PMMA $<$ PE $<$ PEG-g-PS consistent with the observed trends of Φ_{pc}'s. Consequently, PEG-g-PS matrix furnishes more advantageous environment for the ring-cyclization reactions of three diarylethene derivatives studied despite the unfavorable polarity effect.

3.2. Kinetics of photochromic ring-cyclization at 77 K

Fig. 3 shows steady-state fluorescence spectra for **1a** and **2a** at 400 nm excitation and **3a** at 340 nm. The fluorescence maxima show large Stokes shifts with increasing matrix polarity for **1a** and **2a**, whereas those for **3a** show much less Stokes shifts. These trends suggest that the excited states of **1a** and **2a** have more polar structures than that of **3a**, and consequently the formers are more influenced by polar matrix environments. The less polar structure for **3a** may be suggested by the smallest dipole moment of **3a** among the three molecules in the ground states (see Fig. 2).

As shown in Fig. 4a, all the fluorescence spectra were fitted with two gaussian bands representing two fluorescence states: a favorable planar conformer for ring-cyclization and an unfavorable twisted conformer. It is known that the planar conformer (i.e. the photochromic state) is characterized with high fluorescence intensity and fast fluorescence decay while the twisted conformer with low fluorescence intensity and slow fluorescence decay [9]. To determine the photochromic state among two fluorescent states (band 1 and band 2), the fluorescence excitation spectra for all sample-matrix combinations were measured. Fig. 4b shows one of the measured excitation spectra for **1a** in PE matrix monitored at 460 and 580 nm corresponding to the maxima of two gaussian bands. Having greater intensities for 460 nm emission at the entire excitation wavelengths suggests that band 1 corresponds to the emission from the photochromic state. The similar trends for other sample-matrix combinations (not shown here) were observed, confirming that band 1 and band 2 are attributed to the emissions from the planar and twisted conformers, respectively.

Fig. 5 exhibits the typical fluorescence decay curves of **1a**, **2a,** and **3a** measured at various excitation and emission wavelengths in PMMA matrix at 77 K. All the decay curves were then fitted with one or two exponential components. So determined lifetimes and relative intensities of fitted components are summarized in Table 2. The observed wavelength dependence of amplitude ratios, combined with the sub-band structures of the fluorescence spectra (Fig. 4a) suggests that the faster component

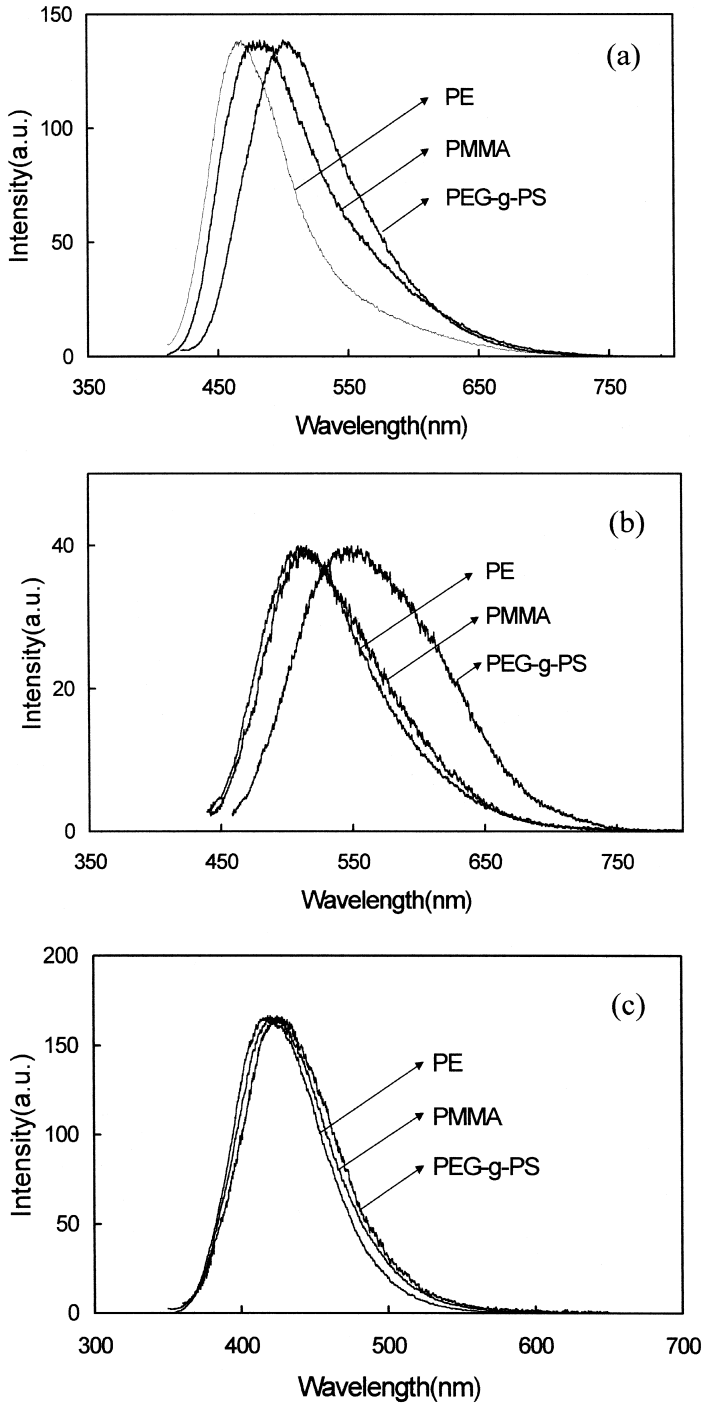

Fig. 3. Steady-state fluorescence spectra of (a) BTCN at excitation wavelength (λ_{ex}) of 400 nm, (b) BTMA at $\lambda_{ex} = 400$ nm, (c) BTF6 at $\lambda_{ex} = 340$ nm.

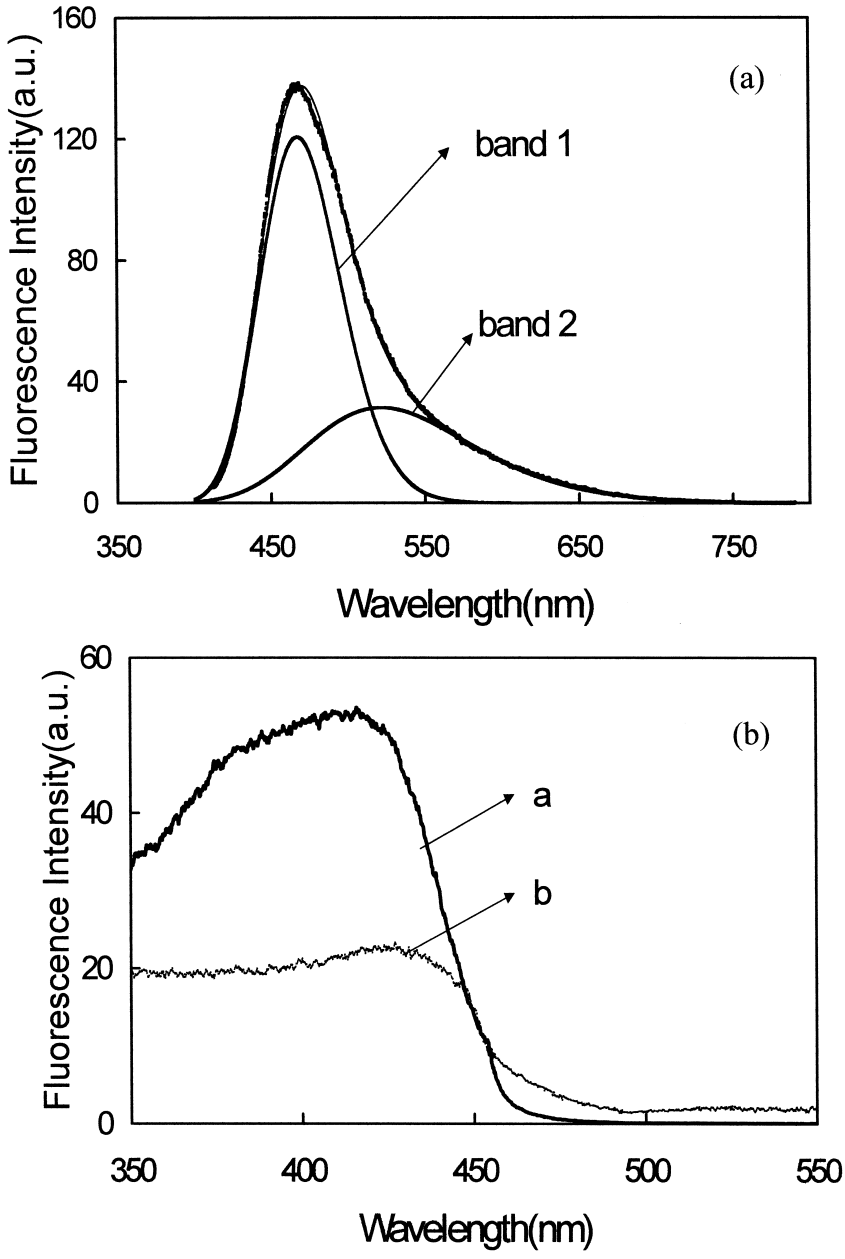

Fig. 4. (a) Sub-band structure of fluorescence spectrum of BTCN in PE. (b) Steady-state fluorescence excitation spectra of BTCN in PE at the detection wavelengths of (a) 460 nm and (b) 580 nm.

($\tau_1 \approx 2.6$ ns except for **2a** in PE and PMMA) is assigned to the favorable planar state for photochromic reaction and the slower component ($\tau_2 \approx 8 \sim 30$ ns) to the unfavorable twisted state. It is noteworthy that the observed lifetimes of **2a** in PE and PMMA ($\tau_1 \approx 5.6$ ns) were more than twice as those of **2a** in PEG-g-PS and others due to the negligible ring-cyclization reactions evidenced by almost zero Φ_{pc}'s for the formers. Assuming that the radiative and nonradiative rate constants are indepen-

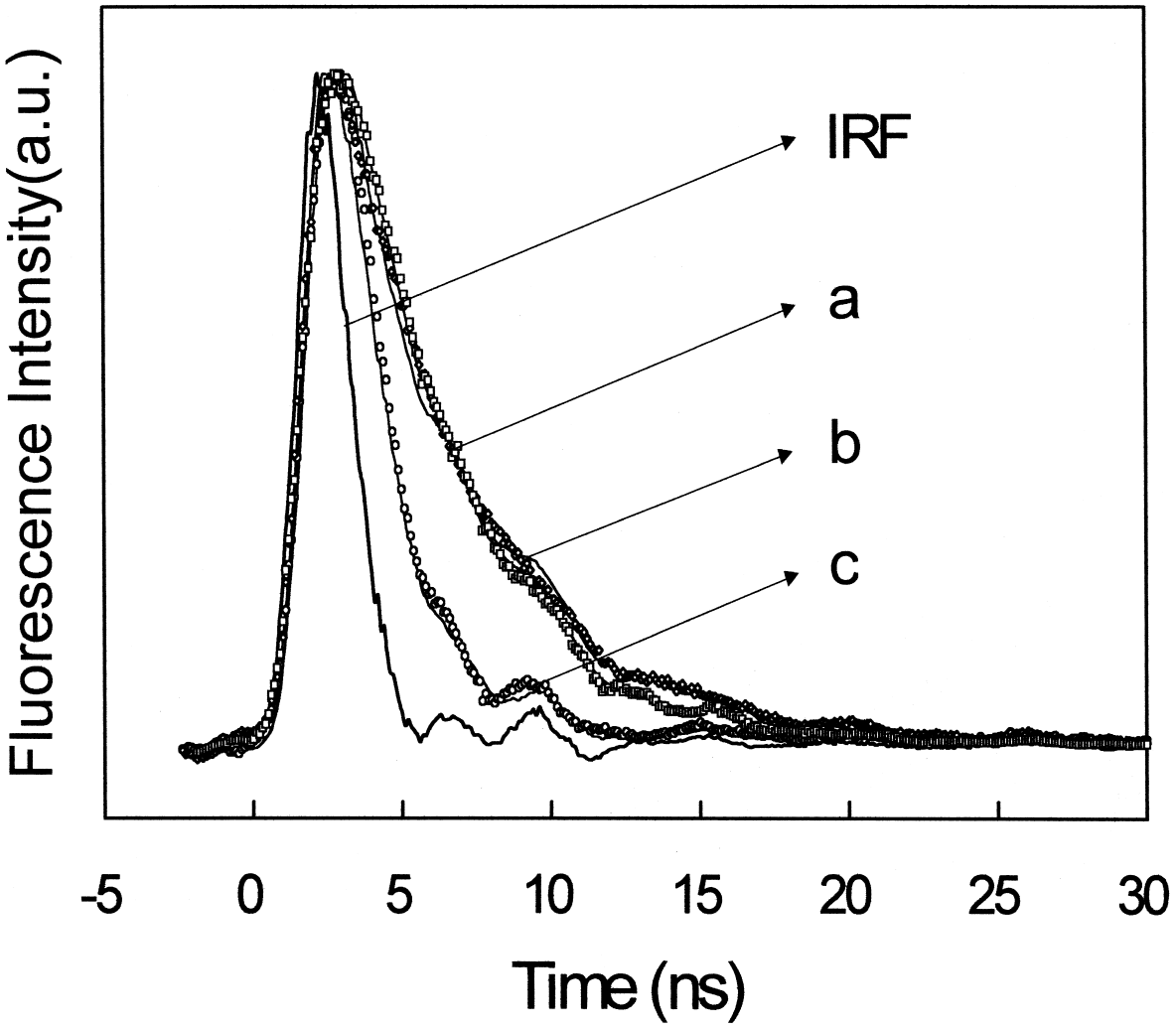

Fig. 5. Fluorescence decay curves at 77 K in PMMA: (a) BTCN (—□—); (b) BTMA (—◇—) at $\lambda_{ex} = 400$ nm, $\lambda_{em} = 475$ nm; (c) BTF6 (—○—) at $\lambda_{ex} = 337$ nm, $\lambda_{em} = 375$ nm. IRF denotes instrument response function. The solid lines along data points are fitted lines.

dent of the types of polymer matrices used, the rate constant of ring-cyclization (k_{cyc}) for **2a** in PEG-g-PS can be easily estimated from the two observed lifetimes for **2a** as in the following:

$$\tau_F = \frac{1}{k_r + k_{nr} + k_{cyc}}, \quad \tau_F' = \frac{1}{k_r + k_{nr}},$$

$$k_{cyc} = \frac{1}{\tau_F} - \frac{1}{\tau_F'}$$

where τ_F, τ_F', k_r, and k_{nr} are the fluorescence lifetime with ring-cyclization reaction, the fluorescence lifetime without ring-cyclization, the radiative rate constant, and the nonradiative rate constant except for the ring-cyclization, respectively. k_{cyc} was calculated to be ~ 0.25 ns^{-1} and the lifetime of ring-cyclization was estimated to be ~ 4.0 ns for **2a** in PEG-g-PS at 77 K. On the other hand, it should be pointed out that the observed lifetimes in the polymer matrices are significantly lengthened from those in the solution phase, and the predicted increases of the contributions from the slower components with the increasing matrix polarity was not seen in present work [9]. The origins of these differences in the

Table 2
Fluorescence lifetimes of BTCN, BTMA, and BTF6 in various matrix films at 77 K

	λ_{em} [a]	τ_1 (ns)	τ_2 (ns)	A_1 / A_2
BTCN,**1a**				
PE	475	2.7		
	550	2.9	8.3	53/47
	600		7.9	
PMMA	475	3.1		
	550	2.9	5.7	49/51
	600		6.8	
PEG-g-PS	500	2.1	7.5	95/5
	550	2.8	10.4	71/29
	600		11.7	
BTMA,**2a**				
PE	500	5.4	11.2	86/14
	550	5.8	10.8	68/32
	625		9.2	
PMMA	500	5.9	11.9	88/12
	550	5.4	11.4	66/34
	625		12.8	
PEG-g-PS	490	2.5		
	550	2.2	9.7	88/12
	600	2.3	9.6	43/57
BTF6,**3a**				
PE	375	2.2		
	425	2.3	15.5	92/8
	500	2.8	13.1	66/34
PMMA	375	2.7		
	425	2.9	35.4	96/4
	500	3.1	36.9	78/22
PEG-g-PS	370	2.0	25.5	96/4
	420	2.5	24.8	94/6
	480	2.6	20.3	70/30

[a] $\lambda_{ex} = 400$ nm for BTCN, BTMA. $\lambda_{ex} = 337$ nm for BTF6.

photochromic dynamics between polymer matrix and solution environments are now under close scrutiny.

4. Conclusions

Photochromic reactions of three diarylethene derivatives embedded in three types of polymer matrices were extensively investigated using a variety of spectroscopic techniques and quantum ab initio computations. It was found that the photochromic efficiencies (Φ_{pc}) of three diarylethene derivatives (**2a** < **1a** < **3a**) are correlated nicely with the structural and electronic characteristics of the Franck–Condon region in the excited states, particularly the dihedral angles of two p orbitals in LUMO of *cis*-hexatriene moieties. At the same time, the photochromic activities are strongly influenced by the environment effects of polymer matrices due to the confined inner free spaces. The conformational changes needed for the photochromic reactions are less hindered with the increasing sizes of free inner spaces (PE < PMMA < PEG-g-PS) correlated with decreasing glass transition temperatures.

The combined steady-state and time-resolved fluorescence studies revealed the details of excited state kinetics involving the radiative and nonradiative processes and the ring-cyclization reactions. The two fluorescence bands centered at the lower and higher wavelengths (e.g. 460 and 580 nm for **1a** in PE) were assigned to the planar and twisted conformers, respectively from the fluorescence excitation spectra and the fluorescence decay curves. The observed fluorescence lifetimes for planar and twisted conformers were ~ 2.6 ns and $8 \sim 30$ ns, respectively, consistent with the previously reported trends in the solution phase that the planar conformer undergoes fast fluorescence decay and the twisted conformer, slow fluorescence decay. Finally, the rate constant of ring-cyclization reaction of **2a** in PEG-g-PS was estimated to be ~ 0.25 ns^{-1} assuming constant radiative and nonradiative rate constants for the three polymer matrices, PE, PMMA, and PEG-g-PS.

Acknowledgements

This work was financially supported by Advanced Photonics Technology Project and CRM-KOSEF grant (1998G0102), Republic of Korea. We thank Sung Kwang Lee for assisting ab initio computation.

References

[1] M. Irie, M. Mohri, J. Org. Chem. 53 (1988) 803.
[2] S. Nakamura, M. Irie, J. Org. Chem. 53 (1988) 6136.
[3] D.A. Parthenopoulos, P.M. Rentzepis, Science 245 (1989) 843.
[4] K. Uchida, Y. Nakayama, M. Irie, Bull. Chem. Soc. Jpn. 63 (1990) 1311.
[5] Y. Nakayama, K. Hayashi, M. Irie, J. Org. Chem. 55 (1990) 2592.
[6] M. Hanazawa, R. Sumiya, Y. Horikawa, M. Irie, J. Chem. Soc., Chem. Commun. (1992) 206.

[7] M. Irie, Pure & Appl. Chem. 68 (1996) 1367.
[8] J. Ern, A.T. Bens, A. Bock, H.D. Martin, C. Kryschi, J. Luminescence 76&77 (1990) 90.
[9] M. Irie, K. Sayo, J. Phys. Chem. 96 (1992) 7671.
[10] H. Miyasaka, S. Araki, A. Tabata, T. Nobuto, N. Mataga, M. Irie, Chem. Phys. Lett. 230 (1994) 249.
[11] N. Tamai, T. Saika, T. Shimidzu, M. Irie, J. Phys. Chem. 100 (1996) 4689.
[12] S.A. Trushin, W. Fuß, T. Schikarski, W.E. Schmid, K.L. Kompa, J. Chem. Phys. 106 (1997) 9386.
[13] H. Miyasaka, T. Nobuto, A. Itaya, N. Tamai, M. Irie, Chem. Phys. Lett. 269 (1997) 281.
[14] G.G. Aloisi, F. Elisei, L. Latterini, U. Mazzucato, M.A. Rogers, J. Am. Chem. Soc. 118 (1996) 10879.
[15] H.P. Stuart, A.A. Neil, A.W. II Larry, J.S. Roseanne, J. Chem. Phys. 107 (1997) 4985.
[16] E. Kim, K.H. Choi, S.B. Rhee, Macromolecules 31 (1998) 5726.
[17] E. Kim, Y.K. Choi, M.H. Lee, Macromolecules 32 (1999) 4855.
[18] M.J. Frisch et al., GAUSSIAN 98, G98W, Gaussian, Inc., Pittsburgh, PA, 1998.
[19] A. Mejiritski, A.Y. Polykarpov, A.M. Sarker, D.C. Neckkers, J. Photochem. Photobiol. 108 (1997) 289.
[20] The detailed geometrical parameters of the optimized structures are available upon request.
[21] A.P. Vladimir, Y.S. Boris, I.M. Vladimir, J. Org. Chem. 57 (1992) 7087.
[22] M.P. Stevens, Polymer Chemistry, Oxford University Press, London, 1990.
[23] J. Brandrup, E.H. Immergut (Eds.) Polymer Handbook, 3nd Ed., John Wiely & Sons, Chichester, 1989.